Field dependent isotropic shifts in solid state nuclear magnetic resonance: A Floquet treatment

Matthew P. Augustine, Kurt W. Zilm, and David B. Zax

Citation: J. Chem. Phys. **98**, 9432 (1993); doi: 10.1063/1.464375
View online: http://dx.doi.org/10.1063/1.464375
View Table of Contents: http://jcp.aip.org/resource/1/JCPSA6/v98/i12
Published by the AIP Publishing LLC.

Field dependent isotropic shifts in solid state nuclear magnetic resonance: A Floquet treatment

Matthew P. Augustine and Kurt W. Zilm
Department of Chemistry, Yale University, 225 Prospect Street, New Haven, Connecticut 06511

David B. Zax
Baker Laboratory, Department of Chemistry, Cornell University, Ithaca, New York 14853-1301

(Received 7 October 1992; accepted 8 December 1992)

The apparent field dependence observed for some isotropic shifts in high resolution solid state NMR is reinvestigated using the Floquet formalism. For ^{13}C–^{1}H systems, second order dipolar shifts are derived that largely agree with the experimental observations made by VanderHart and his theoretical treatment while resolving some difficulties in the use of a secular approximation to handle an inherently time-dependent problem. Additional second order terms are shown to give rise to both frequency shifts and line broadening which can be significant in some spin pairs. This line broadening is found to arise from a second order coupling of the rf field with the I–S dipolar interaction.

INTRODUCTION

In 1986 VanderHart[1] reported an apparent field dependence in the isotropic ^{13}C chemical shifts measured in high resolution solid state NMR spectra of organic solids using high power ^{1}H decoupling[2] and magic angle sample spinning (MASS).[3] While the overall shift differences with field were small, they cast in doubt the suitability of some secondary chemical shift reference materials.[4] One key observation was that the field dependent shifts varied in a consistent fashion with the magnitude of the undecoupled ^{13}C–^{1}H dipolar interaction. Methylene carbon centers displayed the greatest field dependence while smaller shifts were seen for methine sites. Little field dependence was observed in motionally averaged systems such as methyl groups and plastic crystals, or for quaternary carbons. Further measurements indicated that the isotropic shifts approached a limiting value with increasing applied field, $\mathbf{B_0}$, and that the size of the shift in Hz was directly proportional to the square of the ratio of the ^{13}C–^{1}H dipolar coupling divided by $\mathbf{B_0}$.

These observations suggested to VanderHart that the field dependence of the shifts was due to second order corrections to the NMR transition frequencies from nonsecular terms in the heteronuclear dipolar interaction. An exact expression for their effect would require a complete solution to the Schrödinger equation for an I–S spin pair including all secular and nonsecular terms in the Hamiltonian. VanderHart presented an analysis using second order perturbation theory which correctly accounts for the functional dependence of the shift on the dipolar coupling, ω_D, and $\mathbf{B_0}$. One problem with this approach is that seemingly similar interaction representations can produce different results.

These difficulties were already noted in Ref. 1. In this paper we present an alternative theoretical analysis, alluded to at that time, using the Floquet formalism.[5] The advantages of this method are that the results are independent of the basis set chosen; i.e., they do not depend upon a judicious choice of interaction representation, and it is computationally efficient. It is found that all of the nonsecular terms in the heteronuclear dipolar interaction can make important contributions to the observed second order shifts, though their relative sizes depend upon the sums and differences of the Larmor frequencies of the coupled spins. The analysis largely corroborates the conclusions of VanderHart with respect to the commonly encountered case of a ^{13}C coupled to a ^{1}H. For other spin pairs, different dipolar terms may dominate, suggesting that additional effects may be observable experimentally.

THEORY

We begin by considering the I spin resonance of a dipolar coupled I–S spin pair when an rf field, $\mathbf{B_1}$, is applied at the Larmor frequency of the S spin. The laboratory frame Hamiltonian in angular frequency units can be written as

$$\mathcal{H}_L = -\omega_I I_z - \omega_S S_z - 2\omega_{\rm rf}\cos\omega_S t(\gamma I_x + S_x) + \mathcal{H}_D^{I-S}, \qquad (1)$$

where the substitution $\gamma = \gamma_I/\gamma_S$ has been used. It is convenient to cast the dipolar Hamiltonian $\mathcal{H}_D^{I-S}$ in terms of a set of geometric factors Ω_n as follows:

$$\Omega_1 = \omega_D(1-3\cos^2\theta), \qquad \Omega_2 = \frac{\omega_D}{4}(3\cos^2\theta - 1),$$
$$\Omega_3 = \frac{3\omega_D}{2}\sin\theta\cos\theta e^{-i\varphi}, \qquad \Omega_4 = \frac{3\omega_D}{4}\sin^2\theta e^{-2i\varphi}.$$

The polar angles ϑ and φ describe the orientation of the I–S internuclear vector in this frame[6] and $\omega_D = \gamma_I\gamma_S\hbar/\mathbf{r}_{IS}^3$ is the dipolar coupling constant. Using these angular factors we write the laboratory frame Hamiltonian as follows:

 0021-9606/93/129432-12$06.00

$$\mathcal{H}_L = -\omega_I I_z - \omega_S S_z - 2\omega_{rf}(\gamma I_x + S_x)\cos\omega_S t + \Omega_1 I_z S_z + \Omega_2(I_+S_- + I_-S_+) + \Omega_3(I_zS_+ + I_+S_z) + \Omega_3^*(I_-S_z + I_zS_-) + \Omega_4 I_+S_+ + \Omega_4^* I_-S_-. \quad (2)$$

Unfortunately, Eq. (2) is expressed in a frame that mixes time-dependent and time-independent terms of varying size. Traditionally, the effect of the time-dependent decoupling field is clarified by entering a rotating frame representation where the interaction of the applied rf field with the S spins appears time independent. In this frame we can rewrite Eq. (2) as

$$\mathcal{H}_R(t) = e^{-i\omega_S t S_z}\mathcal{H}_L(t)e^{i\omega_S t S_z}$$
$$= -\omega_I I_z - \omega_{rf}S_x + \Omega_1 I_z S_z + \Omega_3 I_+S_z + \Omega_3^* I_-S_z + e^{i\omega_S t}(-\gamma\omega_{rf}I_x + \Omega_2 I_+S_- + \Omega_3^* I_zS_- + \Omega_4^* I_-S_-)$$
$$+ e^{-i\omega_S t}(-\gamma\omega_{rf}I_x + \Omega_2 I_-S_+ + \Omega_3 I_zS_+ + \Omega_4 I_+S_+) - e^{2i\omega_S t}(\frac{\omega_{rf}}{2}S_-) - e^{-2i\omega_S t}(\frac{\omega_{rf}}{2}S_+). \quad (3)$$

The matrix elements of this Hamiltonian are shown in the Appendix. Equation (3) can be used to calculate transition frequencies at several levels of approximation. A basic treatment of Eq. (3) retains only the I_zS_z term of the dipolar interaction reducing Eq. (3) to

$$\mathcal{H}^{(0)} = -\omega_I I_z - \omega_{rf}S_x + \Omega_1 I_z S_z.$$

This Hamiltonian can be written in matrix form in the direct product basis of eigenstates $|m_I,m_S\rangle$ as $\mathcal{H}^{(0)} =$

$$\begin{array}{c} \\ \langle\alpha\alpha| \\ \langle\alpha\beta| \\ \langle\beta\alpha| \\ \langle\beta\beta| \end{array} \begin{array}{c} \begin{array}{cccc} |\alpha\alpha\rangle & |\alpha\beta\rangle & |\beta\alpha\rangle & |\beta\beta\rangle \end{array} \\ \begin{pmatrix} -\frac{\omega_I}{2}+\frac{\Omega_1}{4} & -\frac{\omega_{rf}}{2} & 0 & 0 \\ -\frac{\omega_{rf}}{2} & -\frac{\omega_I}{2}-\frac{\Omega_1}{4} & 0 & 0 \\ 0 & 0 & \frac{\omega_I}{2}-\frac{\Omega_1}{4} & -\frac{\omega_{rf}}{2} \\ 0 & 0 & -\frac{\omega_{rf}}{2} & \frac{\omega_I}{2}+\frac{\Omega_1}{4} \end{pmatrix} \end{array}.$$

Because of the resonant nature of the interaction of the rf field with the spin system, it is inappropriate to treat this portion of the problem using perturbation theory. The matrix $\mathcal{T}$, shown below, transforms $\mathcal{H}^{(0)}$ from the direct product basis into the manifold of states $\{|1\rangle,|2\rangle,|3\rangle,|4\rangle\}$.

$$\mathcal{T} = \begin{array}{c} \\ \langle\alpha\alpha| \\ \langle\alpha\beta| \\ \langle\beta\alpha| \\ \langle\beta\beta| \end{array} \begin{array}{c} \begin{array}{cccc} |1\rangle & |2\rangle & |3\rangle & |4\rangle \end{array} \\ \begin{pmatrix} \cos\xi & \sin\xi & 0 & 0 \\ -\sin\xi & \cos\xi & 0 & 0 \\ 0 & 0 & \cos\xi & -\sin\xi \\ 0 & 0 & \sin\xi & \cos\xi \end{pmatrix} \end{array}.$$

When $\tan 2\xi = 2\omega_{rf}/\Omega_1$ $\mathcal{H}^{(0)}$ becomes diagonal with eigenvalues (in frequency units),

$$E_{|1\rangle} = -\frac{\omega_I}{2} + \frac{\Omega_1}{4}\cos 2\xi + \frac{\omega_{rf}}{2}\sin 2\xi,$$
$$E_{|2\rangle} = -\frac{\omega_I}{2} - \frac{\Omega_1}{4}\cos 2\xi - \frac{\omega_{rf}}{2}\sin 2\xi,$$
$$E_{|3\rangle} = +\frac{\omega_I}{2} - \frac{\Omega_1}{4}\cos 2\xi - \frac{\omega_{rf}}{2}\sin 2\xi,$$
$$E_{|4\rangle} = +\frac{\omega_I}{2} + \frac{\Omega_1}{4}\cos 2\xi + \frac{\omega_{rf}}{2}\sin 2\xi.$$

In the limit of good decoupling ($\xi = \pi/4$) the only allowed transitions are $|1\rangle \rightarrow |4\rangle$ and $|2\rangle \rightarrow |3\rangle$ which are found at the common transition frequency, ω_I.[7] This is the generally accepted understanding of the decoupled transition frequency—in the limit of good decoupling it is independent of the dipolar coupling between the two spins and falls at the chemical shift. Even under less than optimal decoupling conditions, the average of the band formed by the overlap of all the allowed lines falls at the same frequency.

In the good decoupling limit the manifold of states $\{|1\rangle,|2\rangle,|3\rangle,|4\rangle\}$ corresponds to a basis where I_z and S_x are good quantum numbers. Subsequently, we refer to this as the I_zS_x basis.

THE SECOND ORDER SHIFT

The frequency resolution of MASS NMR spectroscopy is sufficient that small line shifts due to terms neglected in the basic treatment can be detected. A better treatment of the Hamiltonian in Eq. (3) would include the effect of as many additional terms as possible. In this spirit, VanderHart suggested[1] that a secular approximation of the type used in time-dependent perturbation theory[8] be applied to suppress only the time-dependent terms in Eq. (3). This Hamiltonian, $\mathcal{H}'$, is found to contain two terms in addition to those considered in the previous section which are proportional to Ω_3 and Ω_3^*.

$$\mathcal{H}' = -\omega_I I_z - \omega_{rf}S_x + \Omega_1 I_z S_z + \Omega_3 I_+S_z + \Omega_3^* I_-S_z,$$

In the I_zS_x basis

$$\mathcal{H}' = \begin{array}{c} \\ \langle 1| \\ \langle 2| \\ \langle 3| \\ \langle 4| \end{array} \begin{array}{c} \begin{array}{cccc} |1\rangle & |2\rangle & |3\rangle & |4\rangle \end{array} \\ \begin{pmatrix} -\frac{\omega_I}{2} + \frac{\Omega_1}{4}\cos 2\xi + \frac{\omega_{rf}}{2}\sin 2\xi & 0 & \frac{\Omega_3}{2} & 0 \\ 0 & -\frac{\omega_I}{2} - \frac{\Omega_1}{4}\cos 2\xi - \frac{\omega_{rf}}{2}\sin 2\xi & 0 & -\frac{\Omega_3}{2} \\ \frac{\Omega_3^*}{2} & 0 & \frac{\omega_I}{2} - \frac{\Omega_1}{4}\cos 2\xi - \frac{\omega_{rf}}{2}\sin 2\xi & 0 \\ 0 & -\frac{\Omega_3^*}{2} & 0 & \frac{\omega_I}{2} + \frac{\Omega_1}{4}\cos 2\xi + \frac{\omega_{rf}}{2}\sin 2\xi \end{pmatrix} \end{array}.$$

Using perturbation theory to treat these new terms, VanderHart recognized that the second order corrections to the zeroth order energies are given by:

$$E_{|q\rangle}^{(2)} = \sum_{p \neq q} \frac{|\langle p|\mathcal{H}'|q\rangle|^2}{E_{|q\rangle} - E_{|p\rangle}} \approx \pm \frac{|\Omega_3|^2}{4\omega_I}.$$

The transition frequencies derived from these energies are proportional to the square of the dipolar interaction and $1/\mathbf{B}_0$, consistent with his experimental observations.

While this treatment reproduces in large measure the experimental observations, it is distressingly dependent on how the problem is formulated. One might equally well choose to treat the problem in the doubly rotating frame[9] where the Ω_3 and Ω_3^* terms again become time dependent. This places them once again on equal footing with the other terms in Eq. (3) that were just previously suppressed. The difficulty is that the type of secular approximation being applied differentiates terms in the Hamiltonian on the basis of their time dependence. Slowly varying terms are kept while rapidly varying terms are discarded. Since the labeling of terms as low frequency or high frequency depends upon the choice of interaction representation, the identity of the terms to be retained is not uniquely defined. When viewed in this context it is appreciated that all of the nonsecular terms must be treated on an equal footing.

This returns us to the apparently intractable problem of solving the complete, time-dependent Schrödinger equation for either Eqs. (2) or (3). Fortunately, the Floquet formalism provides an efficient means of solving problems involving time dependent Hamiltonians.[10]

THE FLOQUET FORMALISM

The time independent Floquet Hamiltonian, H_F, associated with a time dependent Hamiltonian, $\mathcal{H}(t)$, is simply derived from the rules outlined by Goelman, Zax, and Vega[5]

$$\langle i, n|H_F|j, k\rangle = \mathcal{H}_{i,j}^{(n-k)} + n\omega\delta_{k,n}\delta_{i,j} \tag{4}$$

where the $\mathcal{H}_{ij}^{(n-k)}$ are the $(n-k)^{\text{th}}$ time dependent Fourier coefficients coupling spin states $\langle i|$ and $|j\rangle$. The basis set of Floquet states[11] for H_F is constructed by taking the direct product of the spin states and a space of infinite dimension labeled by a Fourier mode index, n. H_F is an

$$\langle \alpha\alpha, n|H_F|\beta\alpha, m\rangle = \begin{array}{c} \\ \vdots \\ \langle \alpha\alpha, 3| \\ \langle \alpha\alpha, 2| \\ \langle \alpha\alpha, 1| \\ \langle \alpha\alpha, 0| \\ \langle \alpha\alpha, -1| \\ \langle \alpha\alpha, -2| \\ \vdots \end{array} \begin{array}{c} \begin{array}{ccccccc} \cdots & |\beta\alpha, 2\rangle & |\beta\alpha, 1\rangle & |\beta\alpha, 0\rangle & |\beta\alpha, -1\rangle & |\beta\alpha, -2\rangle & \cdots \end{array} \\ \begin{pmatrix} \ddots & & & & & & \\ \ddots & -\frac{1}{2}\gamma\omega_{rf} & & & & & \\ \ddots & \frac{1}{2}\Omega_3 & -\frac{1}{2}\gamma\omega_{rf} & & & & \\ & -\frac{1}{2}\gamma\omega_{rf} & \frac{1}{2}\Omega_3 & -\frac{1}{2}\gamma\omega_{rf} & & & \\ & & -\frac{1}{2}\gamma\omega_{rf} & \frac{1}{2}\Omega_3 & -\frac{1}{2}\gamma\omega_{rf} & & \\ & & & -\frac{1}{2}\gamma\omega_{rf} & \frac{1}{2}\Omega_3 & -\frac{1}{2}\gamma\omega_{rf} & \\ & & & & -\frac{1}{2}\gamma\omega_{rf} & \frac{1}{2}\Omega_3 & -\frac{1}{2}\gamma\omega_{rf} \\ & & & & & \ddots & \ddots \end{pmatrix} \end{array}$$

FIG. 1. Expanded version of the $\langle \alpha\alpha,n|H_F|\beta\alpha,k\rangle$ sub-block of the Floquet Hamiltonian.

infinite matrix as n can take on all values from $-\infty$ to $+\infty$. Its diagonal elements are identical to those of $\mathscr{H}(t)$, except for an additional $n\omega$ term which tracks the mode index of the Fourier expansion.

Time dependence of the form $e^{im\omega t}$ in $\mathscr{H}(t)$ corresponds to matrix elements coupling Floquet states whose mode numbers differ by m. The Floquet Hamiltonian, H_F, associated with $\mathscr{H}_R(t)$ [Eq. (3)] is shown below in a compact matrix notation. An expanded version of the $\langle\alpha\alpha,n|H_F|\beta\alpha,k\rangle$ sub-block is given in Fig. 1.

$$
\begin{array}{c}
 \\
\langle\alpha\alpha,n| \\
\langle\alpha\beta,n| \\
\langle\beta\alpha,n| \\
\langle\beta\beta,n|
\end{array}
\begin{array}{c}
\begin{array}{cccc} |\alpha\alpha,k\rangle & |\alpha\beta,k\rangle & |\beta\alpha,k\rangle & |\beta\beta,k\rangle \end{array} \\
\begin{pmatrix}
(-\frac{\omega_I}{2}+\frac{\Omega_1}{4}+n\omega_S)\delta_0 & -\frac{1}{2}[\omega_{rf}(\delta_2+\delta_0)-\Omega_3\delta_1] & -\frac{1}{2}[\gamma\omega_{rf}(\delta_1+\delta_{-1})-\Omega_3\delta_0] & \Omega_4\delta_1 \\
-\frac{1}{2}[\omega_{rf}(\delta_0+\delta_{-2})-\Omega_3^*\delta_{-1}] & (-\frac{\omega_I}{2}-\frac{\Omega_1}{4}+n\omega_S)\delta_0 & \Omega_2\delta_{-1} & -\frac{1}{2}[\gamma\omega_{rf}(\delta_1+\delta_{-1})+\Omega_3\delta_0] \\
-\frac{1}{2}[\gamma\omega_{rf}(\delta_{-1}+\delta_1)-\Omega_3^*\delta_0] & \Omega_2\delta_1 & (\frac{\omega_I}{2}-\frac{\Omega_1}{4}+n\omega_S)\delta_0 & -\frac{1}{2}[\omega_{rf}(\delta_2+\delta_0)+\Omega_3\delta_1] \\
\Omega_4^*\delta_{-1} & -\frac{1}{2}[\gamma\omega_{rf}(\delta_{-1}+\delta_1)+\Omega_3^*\delta_0] & -\frac{1}{2}[\omega_{rf}(\delta_{-2}+\delta_0)+\Omega_3^*\delta_{-1}] & (\frac{\omega_I}{2}+\frac{\Omega_1}{4}+n\omega_S)\delta_0
\end{pmatrix}
\end{array}
$$

The δ_{n-k} functions indicate the presence of element coupling Floquet states in a given sub-block that differ in mode number by $n-k$. The δ_0 components of H_F are just the time-independent elements of $\mathscr{H}_R(t)$ and couple Floquet states where $n=k$. Time-dependent terms in $\mathscr{H}_R(t)$ couple Floquet states where $n\neq k$. These terms are off diagonal in the mode index just as terms in ω_{rf} are off diagonal in the spin eigenstates. Notice that in the Floquet treatment of $\mathscr{H}_R(t)$ terms that are nonsecular in the sense of being small and off diagonal are treated equivalently as those that are nonsecular in the sense of being large, off diagonal, and time dependent.

Our goal is to calculate the eigenvalues of H_F, and thus the NMR transition frequencies. In the strong decoupling limit, a more convenient Floquet basis is formed from the $\{|1\rangle,|2\rangle,|3\rangle,|4\rangle\}$ spin basis and the manifold spanned by the mode index. In analogy to the treatment of $\mathscr{H}^{(0)}$ we define a transformation

$$
\mathcal{T}_F=
\begin{array}{c}
 \\
\langle\alpha\alpha,n| \\
\langle\alpha\beta,n| \\
\langle\beta\alpha,n| \\
\langle\beta\beta,n|
\end{array}
\begin{array}{c}
\begin{array}{cccc} |1,k\rangle & |2,k\rangle & |3,k\rangle & |4,k\rangle \end{array} \\
\begin{pmatrix}
\cos\xi\ \delta_0 & \sin\xi\ \delta_0 & 0 & 0 \\
-\sin\xi\ \delta_0 & \cos\xi\ \delta_0 & 0 & 0 \\
0 & 0 & \cos\xi\ \delta_0 & -\sin\xi\ \delta_0 \\
0 & 0 & \sin\xi\ \delta_0 & \cos\xi\ \delta_0
\end{pmatrix}
\end{array},
$$

where $\xi=\pi/4$ in the limit of good decoupling. The matrix elements of the transformed H_F can be written in the usual fashion[12]

$$
\langle j,n|H_F|k,m\rangle=\sum_{l,l'}\langle j,n|\mathcal{T}_F^{-1}|l,n\rangle\langle l,n|H_F|l',m\rangle \times\langle l',m|\mathcal{T}_F|k,m\rangle,
$$

where j, k, or l refer to states of the I–S spin system and n and m are Fourier mode indices.

THE FLOQUET SECOND ORDER SHIFT

The Floquet matrix expressed in the I_zS_x basis set is presented in Fig. 2. As all the off-diagonal elements in H_F are small in comparison to the difference in diagonal elements between coupled states the effect of these cross terms can be calculated using the standard methods of nondegenerate perturbation theory. The second order line shifts can be calculated using

$$
E^{(2)}_{|q,m\rangle}=\sum_{p\neq q}\sum_{l=-\infty}^{\infty}\frac{|\langle p,l|H_F|q,m\rangle|^2}{E_{|q,m\rangle}-E_{|p,l\rangle}}.
$$

The second order perturbation corrections to the eigenvalues of H_F are independent of mode number because both the energy differences and the off-diagonal terms depend upon the Fourier mode indices only through the difference $l-m$. The second order eigenvalue corrections (in the standard limit that $\omega_I\gg\Omega_1,\omega_{rf}$) are given below.

$$
E^{(2)}_{|1,\ell\rangle}=-E^{(2)}_{|4,\ell\rangle}=-\frac{\cos 2\xi}{8\omega_S}(\omega_{rf}^2+2|\Omega_3|^2)-\frac{1}{4(\omega_I-\omega_S)}[4\sin^2\xi|\Omega_2|^2+\gamma^2\omega_{rf}^2+2\gamma\omega_{rf}\sin 2\xi\ \Omega_2]
$$
$$
-\frac{|\Omega_3|^2}{4\omega_I}-\frac{1}{4(\omega_I+\omega_S)}[4\cos^2\xi|\Omega_4|^2+\gamma^2\omega_{rf}^2+\gamma\omega_{rf}\sin 2\xi(\Omega_4+\Omega_4^*)]
$$

$$
E^{(2)}_{|2,\ell\rangle}=-E^{(2)}_{|3,\ell\rangle}=\frac{\cos 2\xi}{8\omega_S}(\omega_{rf}^2+2|\Omega_3|^2)-\frac{1}{4(\omega_I-\omega_S)}[4\cos^2\xi|\Omega_2|^2+\gamma^2\omega_{rf}^2-2\gamma\omega_{rf}\sin 2\xi\ \Omega_2]
$$
$$
-\frac{|\Omega_3|^2}{4\omega_I}-\frac{1}{4(\omega_I+\omega_S)}[4\sin^2\xi|\Omega_4|^2+\gamma^2\omega_{rf}^2-\gamma\omega_{rf}\sin 2\xi(\Omega_4+\Omega_4^*)]
$$

$$
H_F = \begin{array}{c} \\ \vdots \\ \langle 1\ n+2| \\ \langle 1\ n+1| \\ \langle 1\ \ n\ \ | \\ \langle 1\ n-1| \\ \langle 1\ n-2| \\ \vdots \\ \langle 2\ n+2| \\ \langle 2\ n+1| \\ \langle 2\ \ n\ \ | \\ \langle 2\ n-1| \\ \langle 2\ n-2| \\ \vdots \\ \langle 3\ n+2| \\ \langle 3\ n+1| \\ \langle 3\ \ n\ \ | \\ \langle 3\ n-1| \\ \langle 3\ n-2| \\ \vdots \\ \langle 4\ n+2| \\ \langle 4\ n+1| \\ \langle 4\ \ n\ \ | \\ \langle 4\ n-1| \\ \langle 4\ n-2| \\ \vdots \end{array}
\begin{pmatrix}
\cdots & |1\ n\rangle & \cdots & |2\ n\rangle & \cdots & |3\ n\rangle & \cdots & |4\ n\rangle & \cdots \\
 & & & & & & & & \\
 & \frac{\omega_{rf}}{4}\sin 2\xi & & \frac{\omega_{rf}}{2}\sin^2\xi & & & & & \\
 & -\frac{\Omega_3^*}{4}\sin 2\xi & & -\frac{\Omega_3^*}{2}\sin^2\xi & & -\frac{\Omega_2}{2}\sin 2\xi-\frac{\gamma\omega_{rf}}{2}\cos 2\xi & & \Omega_2\sin^2\xi+\frac{\gamma\omega_{rf}}{2}\sin 2\xi & \\
 & -\frac{\omega_I}{2}+n\omega_S+\frac{\Omega_1}{4}\cos 2\xi+\frac{\omega_{rf}}{2}\sin 2\xi & & & & \frac{\Omega_3}{2} & & & \\
 & -\frac{\Omega_3}{4}\sin 2\xi & & \frac{\Omega_3}{2}\cos^2\xi & & \frac{\Omega_4}{2}\sin 2\xi-\frac{\gamma\omega_{rf}}{2}\cos 2\xi & & \Omega_4\cos^2\xi+\frac{\gamma\omega_{rf}}{2}\sin 2\xi & \\
 & \frac{\omega_{rf}}{4}\sin 2\xi & & -\frac{\omega_{rf}}{2}\cos^2\xi & & & & & \\
 & & & & & & & & \\
 & -\frac{\omega_{rf}}{2}\cos^2\xi & & -\frac{\omega_{rf}}{4}\sin 2\xi & & & & & \\
 & \frac{\Omega_3^*}{2}\cos^2\xi & & \frac{\Omega_3^*}{4}\sin 2\xi & & \Omega_2\cos^2\xi-\frac{\gamma\omega_{rf}}{2}\sin 2\xi & & \frac{-\Omega_2}{2}\sin 2\xi-\frac{\gamma\omega_{rf}}{2}\cos 2\xi & \\
 & & & -\frac{\omega_I}{2}+n\omega_S-\frac{\Omega_1}{4}\cos 2\xi-\frac{\omega_{rf}}{2}\sin 2\xi & & & & -\frac{\Omega_3}{2} & \\
 & -\frac{\Omega_3}{2}\sin^2\xi & & \frac{\Omega_3}{4}\sin 2\xi & & \Omega_4\sin^2\xi-\frac{\gamma\omega_{rf}}{2}\sin 2\xi & & \frac{\Omega_4}{2}\sin 2\xi-\frac{\gamma\omega_{rf}}{2}\cos 2\xi & \\
 & \frac{\omega_{rf}}{2}\sin^2\xi & & -\frac{\omega_{rf}}{4}\sin 2\xi & & & & & \\
 & & & & & & & & \\
 & & & & & -\frac{\omega_{rf}}{4}\sin 2\xi & & \frac{\omega_{rf}}{2}\sin^2\xi & \\
 & \frac{\Omega_4^*}{2}\sin 2\xi-\frac{\gamma\omega_{rf}}{2}\cos 2\xi & & \Omega_4^*\sin^2\xi-\frac{\gamma\omega_{rf}}{2}\sin 2\xi & & -\frac{\Omega_3^*}{4}\sin 2\xi & & \frac{\Omega_3^*}{2}\sin^2\xi & \\
 & \frac{\Omega_3^*}{2} & & & & \frac{\omega_I}{2}+n\omega_S-\frac{\Omega_1}{4}\cos 2\xi-\frac{\omega_{rf}}{2}\sin 2\xi & & & \\
 & -\frac{\Omega_2}{2}\sin 2\xi-\frac{\gamma\omega_{rf}}{2}\cos 2\xi & & \Omega_2\cos^2\xi-\frac{\gamma\omega_{rf}}{2}\sin 2\xi & & -\frac{\Omega_3}{4}\sin 2\xi & & -\frac{\Omega_3}{2}\cos^2\xi & \\
 & & & & & -\frac{\omega_{rf}}{4}\sin 2\xi & & -\frac{\omega_{rf}}{2}\cos^2\xi & \\
 & & & & & & & & \\
 & & & & & -\frac{\omega_{rf}}{2}\cos^2\xi & & \frac{\omega_{rf}}{4}\sin 2\xi & \\
 & \Omega_4^*\cos^2\xi+\frac{\gamma\omega_{rf}}{2}\sin 2\xi & & \frac{\Omega_4^*}{2}\sin 2\xi-\frac{\gamma\omega_{rf}}{2}\cos 2\xi & & -\frac{\Omega_3^*}{2}\cos^2\xi & & \frac{\Omega_3^*}{4}\sin 2\xi & \\
 & & & -\frac{\Omega_3^*}{2} & & & & \frac{\omega_I}{2}+n\omega_S+\frac{\Omega_1}{4}\cos 2\xi+\frac{\omega_{rf}}{2}\sin 2\xi & \\
 & \Omega_2\sin^2\xi+\frac{\gamma\omega_{rf}}{2}\sin 2\xi & & -\frac{\Omega_2}{2}\sin 2\xi-\frac{\gamma\omega_{rf}}{2}\cos 2\xi & & \frac{\Omega_3}{2}\sin^2\xi & & \frac{\Omega_3}{4}\sin 2\xi & \\
 & & & & & \frac{\omega_{rf}}{2}\sin^2\xi & & \frac{\omega_{rf}}{4}\sin 2\xi & \\
 & & & & & & & &
\end{pmatrix}
$$

FIG. 2. Matrix representation of H_F in the I_zS_x spin basis.

Selection rules that determine the observed NMR spectrum are, as usual, governed by the matrix elements of I_x. Transforming into the I_zS_x Floquet basis this operator is

$$
I_x = \begin{array}{c} \\ \langle 1,n| \\ \langle 2,n| \\ \langle 3,n| \\ \langle 4,n| \end{array}
\begin{pmatrix}
|1,k\rangle & |2,k\rangle & |3,k\rangle & |4,k\rangle \\
0 & 0 & \cos 2\xi\ \delta_0 & -\sin 2\xi\ \delta_0 \\
0 & 0 & \sin 2\xi\ \delta_0 & \cos 2\xi\ \delta_0 \\
\cos 2\xi\ \delta_0 & \sin 2\xi\ \delta_0 & 0 & 0 \\
-\sin 2\xi\ \delta_0 & \cos 2\xi\ \delta_0 & 0 & 0
\end{pmatrix}.
$$

The states coupled by nonzero elements of I_x correspond to allowed transitions.[13] Under conditions of good decoupling $\cos 2\xi \approx 0$ and $\sin 2\xi \approx 1$ and the only allowed transitions are $|1,k\rangle \rightarrow |4,k\rangle$ at frequency $\Delta\omega_{41}$ and $|2,k\rangle \rightarrow |3,k\rangle$ at frequency $\Delta\omega_{32}$. Additional transitions between $\Delta k \neq 0$ Floquet states are also present and are displaced about the $k=0$ transition by $\pm k\omega_S$. The intensity of these satellite transitions is vanishingly small in the high field limit, and therefore are not relevant to the present problem.

The corrected transition frequencies are calculated as

$$
\begin{aligned}
\Delta\omega_{41} = \omega_I &+ \frac{1}{2\omega_I}|\Omega_3|^2 \\
&+ \frac{1}{2(\omega_I+\omega_S)}[2|\Omega_4|^2+\gamma^2\omega_{rf}^2+\gamma\omega_{rf}(\Omega_4+\Omega_4^*)] \\
&+ \frac{1}{2(\omega_I-\omega_S)}[2|\Omega_2|^2+\gamma^2\omega_{rf}^2+2\gamma\omega_{rf}\ \Omega_2] \qquad (5)
\end{aligned}
$$

$$
\begin{aligned}
\Delta\omega_{32} = \omega_I &+ \frac{1}{2\omega_I}|\Omega_3|^2 \\
&+ \frac{1}{2(\omega_I+\omega_S)}[2|\Omega_4|^2+\gamma^2\omega_{rf}^2-\gamma\omega_{rf}(\Omega_4+\Omega_4^*)] \\
&+ \frac{1}{2(\omega_I-\omega_S)}[2|\Omega_2|^2+\gamma^2\omega_{rf}^2-2\gamma\omega_{rf}\ \Omega_2] \qquad (6)
\end{aligned}
$$

Under actual experimental conditions one would not generally resolve each transition separately. In most cases, all that will be observed is an average transition frequency

$$\omega_{av} = \omega_I + \frac{1}{2\omega_I}|\Omega_3|^2 + \frac{1}{2(\omega_I+\omega_S)}[2|\Omega_4|^2 + \gamma^2\omega_{rf}^2] + \frac{1}{2(\omega_I-\omega_S)}[2|\Omega_2|^2 + \gamma^2\omega_{rf}^2] \quad (7)$$

with excess width

$$\Delta\omega_{\pm} = \gamma\omega_{rf}\left(\frac{(\Omega_4+\Omega_4^*)}{\omega_I+\omega_S} + \frac{2\Omega_2}{\omega_I-\omega_S}\right) \quad (8)$$

While the formalism requires the use of a particular rotating frame representation, each of the off-diagonal terms in the dipolar Hamiltonian has been treated equivalently, and each makes some contribution to the second order dipolar shift. It has been verified that the shifts calculated in Eqs. (5)–(7) are independent to this order of perturbation of the zeroth order basis.

The average transition frequency appears shifted from the *chemical shift* frequency, ω_I, by a series of terms which depend upon the square of the dipole–dipole coupling divided by ω_I, $\omega_I+\omega_S$ or $\omega_I-\omega_S$. Additionally, shifts are observed proportional to ω_{rf}^2 which are the well known off resonance Bloch–Siegert shift. Since these shift all I spin resonances equally,[14] they do not affect shift differences measured relative to a secondary reference standard. The terms proportional to $|\Omega_3|^2$ comprise the dipolar coupling dependent second order shift identified by VanderHart.[1] In this treatment there are new contributions from $|\Omega_2|^2$ and $|\Omega_4|^2$. Which term dominates depends upon the sizes of the energy denominators ω_I, $\omega_I+\omega_S$, and $\omega_I-\omega_S$ and the orientation of $\mathbf{r}_{IS}$ with respect to $\mathbf{B}_0$.

The linewidth surprisingly depends not only on the size of dipole–dipole couplings, but on the strength of the decoupling field, ω_{rf}, via a new mechanism which is not Bloch–Siegert like. This effect could be significant in spin systems where the sum or difference in Larmor frequencies is small. These frequency dependences are best illustrated by considering the powder line shapes calculated from Eqs. (5) and (6).

STATIC LINE SHAPES WITH DECOUPLING

The line shapes resulting from these formulas were obtained using a computer program to step over the polar angles present Eqs. (5) and (6) in a standard fashion. Figure 3 shows the patterns for methine ^{13}C–^{1}H pairs having $\omega_D/2\pi=23$ kHz (which is appropriate for a spin separation of 1.09 Å) and $\omega_{rf}/2\pi$ set to (a) 40 kHz and (b) 100 kHz. *Pseudo-power* broadening is clearly illustrated by comparing the widths of the transitions at different decoupling field amplitudes, i.e., the full width (FW) of the line shape increases from 18 to 25 Hz upon increasing $\omega_{rf}/2\pi$ from 40 to 100 kHz. Figure 4 shows the expected dipolar spectra for a ^{119}Sn–^{1}H spin pair found in $SnHR_3$ with $\omega_D/2\pi=8.7$ kHz resulting from a spin separation of 1.71 Å and using the same decoupling field strengths as mentioned above. These line shapes also confirm the presence of the pseudo-power broadening mechanism.

Unfortunately these line shapes could only be observed in the absence of chemical shift anisotropy (CSA). The existence of the pseudo-power broadening would probably best be observed in small molecules dissolved in a nematic phase or in single crystals where the linewidths are naturally small because the average orientation of all molecules is identical. Thus, it may prove possible to observe the differential broadening predicted by Eq. (8) above as a power dependent resonance shift in these cases. Equations (7) and (8) indicate that the lineshift depends upon terms of the form $|\Omega_n|^2$ while the pseudo-power broadening depends upon $\Omega_n\omega_{rf}$. Since the effects being considered here will be obscured by the CSA in powdered samples it is most informative to consider the line shapes that will be obtained with magic angle sample spinning.

DECOUPLING WITH MAGIC ANGLE SPINNING

It will prove helpful to reexpress the results derived above in a form which better emphasizes rotational prop-

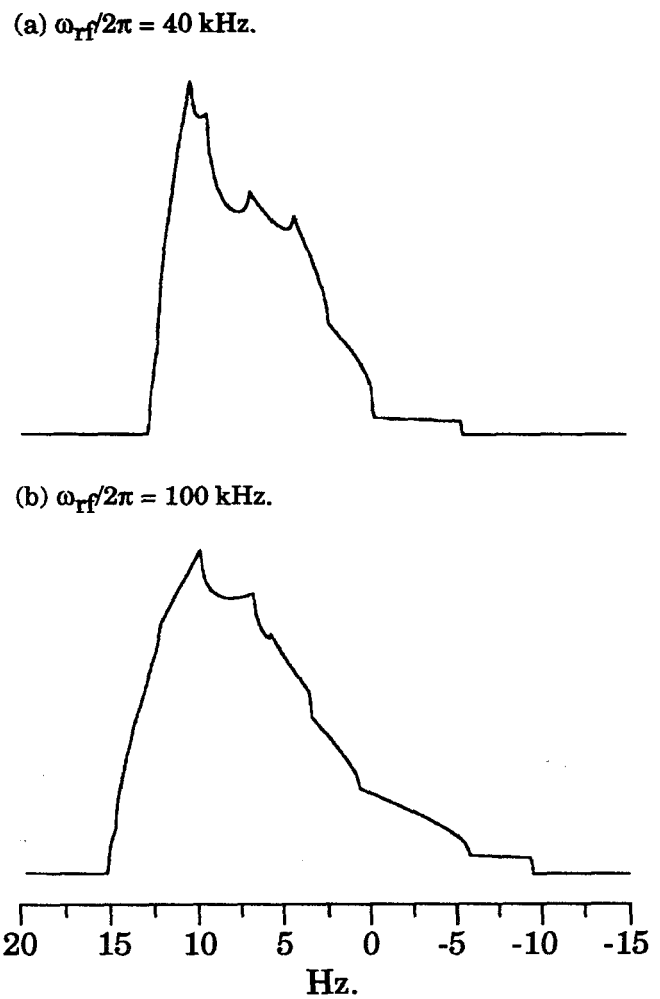

FIG. 3. Expected dipolar spectra assuming no CSA at B=1.4 T for methine ^{13}C–^{1}H pairs separated by 1.09 Å. The FW of the line shapes increase from (a) 18 Hz at $\omega_{rf}/2\pi=40$ kHz to (b) 25 Hz at $\omega_{rf}/2\pi=100$ kHz.

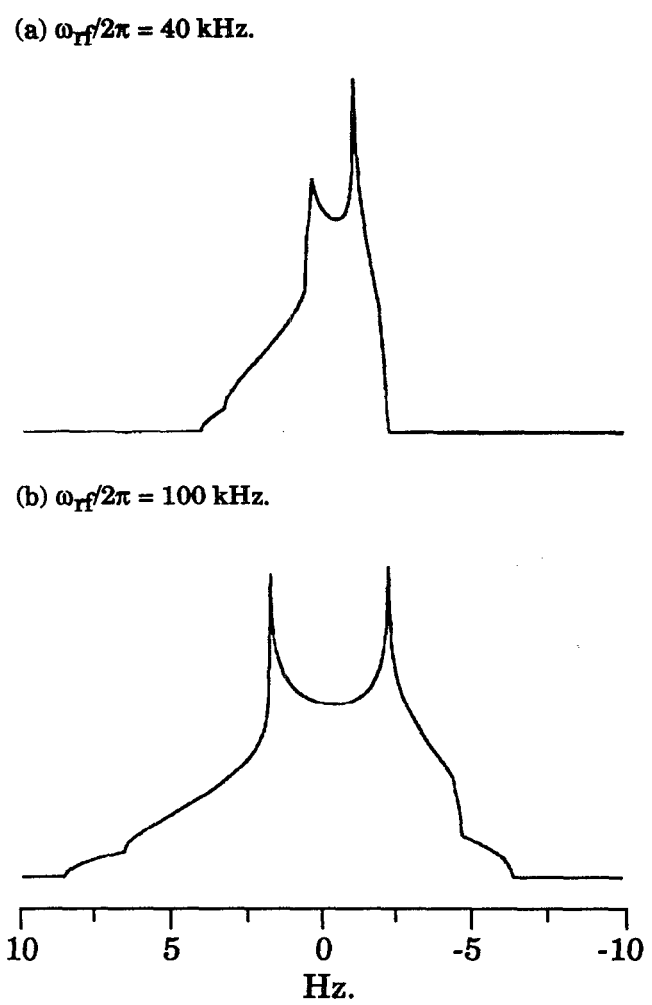

FIG. 4. Simulated dipolar line shapes again assuming no CSA at B=1.4 T for the ^{119}Sn–^{1}H spin pair found in $SnHR_3$. The FW of the line shape increases from (a) 6 Hz at $\omega_{rf}/2\pi$=40 kHz to (b) 15 Hz at $\omega_{rf}/2\pi$=100 kHz.

erties, i.e., by rewriting the terms which depend upon angular factors in terms of the Wigner rotation matrices by using vector coupling coefficients. The relevant angular factors are

$$\begin{aligned}
\Omega_2 &= \frac{\omega_D}{2} d_{00}^{(2)}(\theta), \\
\Omega_4 + \Omega_4^* &= -\sqrt{6}\omega_D d_{02}^{(2)}(\theta)\cos 2\varphi, \\
|\Omega_2|^2 &= \frac{\omega_D^2}{140}(18 d_{00}^{(4)}(\theta) + 10 d_{00}^{(2)}(\theta) + 7), \\
|\Omega_3|^2 &= \frac{3\omega_D^2}{70}(-12 d_{00}^{(4)}(\theta) + 5 d_{00}^{(2)}(\theta) + 7), \\
|\Omega_4|^2 &= \frac{3\omega_D^2}{70}(3 d_{00}^{(4)}(\theta) - 10 d_{00}^{(2)}(\theta) + 7).
\end{aligned} \tag{9}$$

The reduced rotation matrices used above have their usual meaning, i.e., $d_{00}^{(2)}(\vartheta) = (3\cos^2\vartheta - 1)/2$, $d_{02}^{(2)}(\vartheta) = (3/8)^{1/2}\sin^2\vartheta$, and $d_{00}^{(4)}(\vartheta) = (3 - 30\cos^2\vartheta + 35\cos^4\vartheta)/8$. In this form we emphasize that there are isotropic, second and fourth rank tensors contributing to the angular dependence of each of the terms of the second order dipolar shift. In powder samples the isotropic component corresponds to a shift in the center of gravity of the resonance line, while the second and fourth rank tensorial components contribute to orientational broadening. The additional pseudo-power broadening mentioned above is purely second rank and depends upon a linear combination of terms which transform in space as $T_0^{(2)}$ from the $\Omega_2\omega_{rf}$ terms and as $T_{\pm 2}^{(2)}$ from the $(\Omega_4 + \Omega_4^*)\ \omega_{rf}$ terms.

The transition frequencies in Eqs. (5) and (6) can be rewritten in terms of reduced matrix elements in order to more fully illustrate the result of different choices of ω_I, ω_S, and ω_{rf} on the static line shape

$$\begin{aligned}
\Delta\omega_{41} = \omega_I &+ \frac{\omega_D^2}{20}\left(\frac{3}{\omega_I} + \frac{6}{\omega_I + \omega_S} + \frac{1}{\omega_I - \omega_S}\right) + \frac{9\omega_D^2}{70}\left(-\frac{2}{\omega_I} + \frac{1}{\omega_I + \omega_S} + \frac{1}{\omega_I - \omega_S}\right) d_{00}^{(4)}(\theta) \\
&- \frac{\sqrt{6}\gamma\omega_{rf}\omega_D}{2(\omega_I + \omega_S)} d_{02}^{(2)}(\theta)\cos 2\varphi + \frac{\omega_D^2}{28}\left(\frac{3}{\omega_I} - \frac{12}{\omega_I + \omega_S} + \frac{2}{\omega_I - \omega_S} + \frac{2\gamma\omega_{rf}}{\omega_D(\omega_I - \omega_S)}\right) d_{00}^{(2)}(\theta), \\
\Delta\omega_{32} = \omega_I &+ \frac{\omega_D^2}{20}\left(\frac{3}{\omega_I} + \frac{6}{\omega_I + \omega_S} + \frac{1}{\omega_I - \omega_S}\right) + \frac{9\omega_D^2}{70}\left(-\frac{2}{\omega_I} + \frac{1}{\omega_I + \omega_S} + \frac{1}{\omega_I - \omega_S}\right) d_{00}^{(4)}(\theta) \\
&+ \frac{\sqrt{6}\gamma\omega_{rf}\omega_D}{2(\omega_I + \omega_S)} d_{02}^{(2)}(\theta)\cos 2\varphi + \frac{\omega_D^2}{28}\left(\frac{3}{\omega_I} - \frac{12}{\omega_I + \omega_S} + \frac{2}{\omega_I - \omega_S} - \frac{2\gamma\omega_{rf}}{\omega_D(\omega_I - \omega_S)}\right) d_{00}^{(2)}(\theta).
\end{aligned}$$

The consequences of MASS on the centerband line shape can be quite simply described using the reduced rotation matrices and some simple geometry. The angles ϑ and φ describing the relative orientation of the internuclear vector, $\mathbf{r}_{IS}$, in the laboratory frame of reference, are made time dependent by mechanically rotating the sample about some axis. We define ζ as the angle that the sample is being rotated about with respect to $\mathbf{B}_0$, $\omega_r t + \alpha_0$ as the (time

dependent) angle swept out during rotation and η as the angle between the rotation axis and the internuclear vector, $\mathbf{r}_{IS}$. It can be shown using direction cosines that

$$\cos(\theta(t)) = \cos\zeta\cos\eta - \sin\zeta\sin\eta\cos(\omega_r t + \alpha_0)$$

and

$$\sin(\theta(t)) = \sin\zeta\cos\eta + \cos\zeta\sin\eta\cos(\omega_r t + \alpha_0)$$

with similar expressions for $\sin[\varphi(t)]$ and $\cos[\varphi(t)]$. The magic angle centerband or isotropic band corresponds to the time averaged transition frequency and requires that we analyze for the time independent portion of the trigonometric functions $d_{00}^{(4)}[\vartheta(t)]$, $d_{00}^{(2)}[\vartheta(t)]$, and $d_{02}^{(2)}[\vartheta(t)]\cos[2\varphi(t)]$. Straightforward algebraic manipulation yields

$$\begin{aligned}\langle d_{00}^{(2)}(\theta(t))\rangle_t &= d_{00}^{(2)}(\zeta)d_{00}^{(2)}(\eta),\\ \langle d_{00}^{(4)}(\theta(t))\rangle_t &= d_{00}^{(4)}(\zeta)d_{00}^{(4)}(\eta),\\ \langle d_{02}^{(2)}(\theta(t))\cos 2\varphi(t)\rangle_t &= d_{02}^{(2)}(\zeta)d_{00}^{(2)}(\eta).\end{aligned}$$

All interactions proportional to $d_{00}^{(2)}[\vartheta(t)]$, including CSA, are averaged to zero when the sample is rotated about the conventional magic angle, which is equivalent to choosing $3\cos^2\zeta - 1 = 0$. At this sample orientation, the other geometric factors are scaled to $-7/18$ for $d_{00}^{(4)}[\vartheta(t)]$ and to $6^{-1/2}$ for $d_{02}^{(2)}[\vartheta(t)]\cos[2\varphi(t)]$ dependence. The transition frequencies for the MASS centerband ($\zeta = 54.74°$) associated with a particular set of orientations described by η in this instance are shown below.

$$\begin{aligned}\Delta\omega_{41} = \omega_I &+ \frac{\omega_D^2}{20}\left(\frac{3}{\omega_I} + \frac{6}{\omega_I+\omega_S} + \frac{1}{\omega_I-\omega_S}\right)\\ &+ \frac{\omega_D^2}{20}\left(\frac{2}{\omega_I} - \frac{1}{\omega_I+\omega_S} - \frac{1}{\omega_I-\omega_S}\right)d_{00}^{(4)}(\eta)\\ &- \frac{\gamma\omega_{\rm rf}\omega_D}{2(\omega_I+\omega_S)}d_{00}^{(2)}(\eta),\end{aligned} \tag{10}$$

$$\begin{aligned}\Delta\omega_{32} = \omega_I &+ \frac{\omega_D^2}{20}\left(\frac{3}{\omega_I} + \frac{6}{\omega_I+\omega_S} + \frac{1}{\omega_I-\omega_S}\right)\\ &+ \frac{\omega_D^2}{20}\left(\frac{2}{\omega_I} - \frac{1}{\omega_I+\omega_S} - \frac{1}{\omega_I-\omega_S}\right)d_{00}^{(4)}(\eta)\\ &+ \frac{\gamma\omega_{\rm rf}\omega_D}{2(\omega_I+\omega_S)}d_{00}^{(2)}(\eta).\end{aligned} \tag{11}$$

Equations (10) and (11) predict that, for powder samples, the MASS centerband will be a superposition of powder patterns resulting from the two separate transitions. Powder patterns are observed under conditions of MASS only in more unusual circumstances, for example, in the homonuclear dipole–dipole coupled systems where the frequency separation between coupled spins matches the spinning rate,[15] and, more routinely, in quadrupolar systems where second order quadrupolar broadening dominates the observed spectrum.[16] These second order quadrupolar powder patterns are similar to those encountered here as they also depend upon both $d_{00}^{(2)}(\eta)$ and $d_{00}^{(4)}(\eta)$. In these situations, the first order second rank interactions are averaged under MASS leaving a magic angle spun powder pattern which depends only on $d_{00}^{(4)}(\eta)$. These second order effects can be averaged away completely by spinning about a second axis magic for $d_{00}^{(4)}(\eta)$. Our powder patterns are an unusual type, they are predicted to depend upon three different geometric functions, $d_{00}^{(2)}(\eta)$, $d_{00}^{(4)}(\eta)$, and $d_{02}^{(2)}(\eta)$. Complete removal of all second order broadening would require simultaneous spinning about three separate axes *magic* for each of these functions.

MASS centerbands for the methine ^{13}C–^{1}H and the ^{119}Sn–^{1}H spin pairs with the same dipolar coupling con-

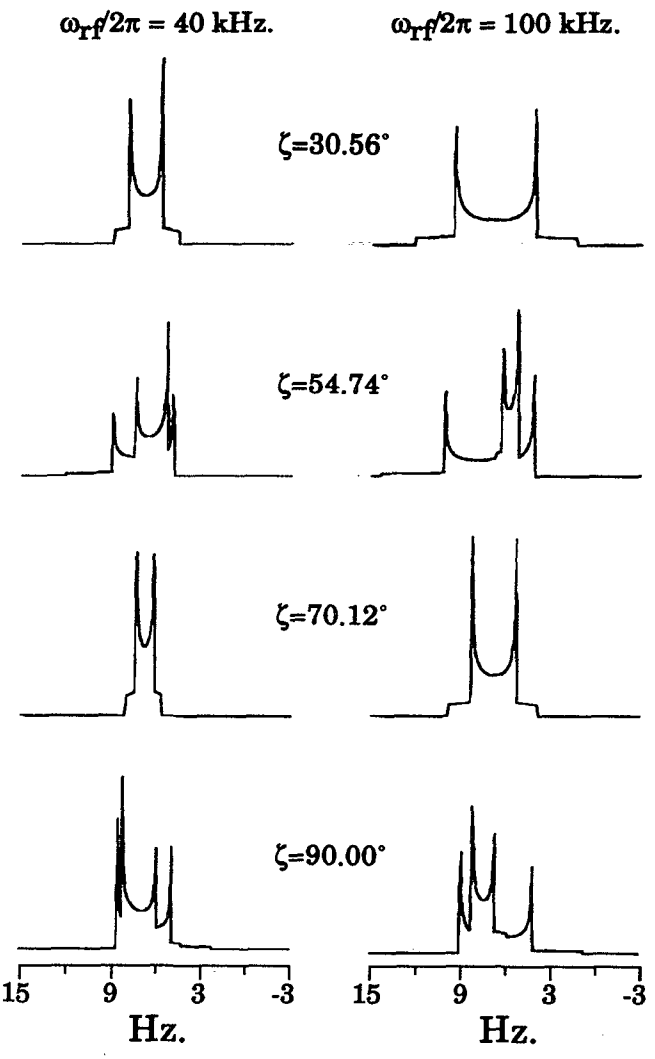

FIG. 5. VASS centerband simulations at $\mathbf{B}=1.4$ T for methine ^{13}C–^{1}H pairs having $\zeta=30.56°$, 54.74°, 70.12°, and 90° and $\omega_{\rm rf}/2\pi=40$ and 100 kHz. The line shapes indicate that the pseudo-power broadening survives sample rotation. The centerbands corresponding to sample rotation at $\zeta=30.56°$ and 70.12° are narrower than those obtained under normal MASS conditions ($\zeta=54.74°$).

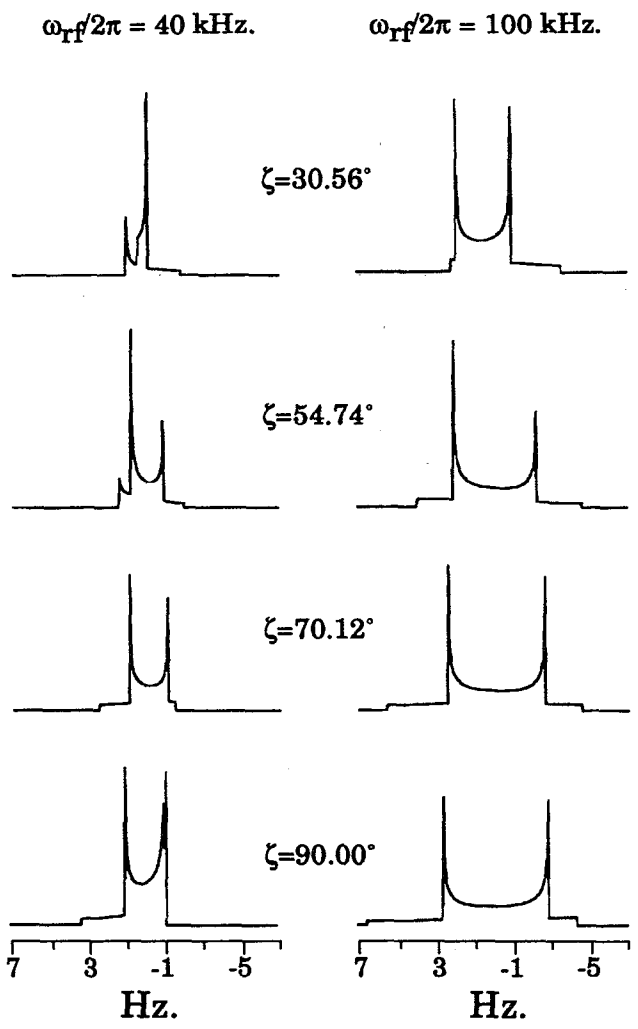

FIG. 6. VASS centerband line shapes at $\mathbf{B}=1.4$ T and with no CSA for the ^{119}Sn–^{1}H spin pair found in $SnHR_3$ having $\zeta=30.56°$, 54.74°, 70.12°, and 90° and $\omega_{rf}/2\pi=40$ and 100 kHz. Again, the pseudo-power broadening is readily evident.

stants mentioned above are shown in Figs. 5 and 6. These figures illustrate two important features of Eqs. (5) and (6) under conditions of MASS. Firstly, the pseudo-power broadening survives sample rotation. For example, in the ^{119}Sn–^{1}H case under normal MASS conditions ($\zeta=54.74°$) the FW of the centerband increases from 3 to 9 Hz upon increasing the decoupling field from 40 to 100 kHz. This increase clearly results from the second rank coupling of the rf field with the dipolar coupling of the two spins, since the dominant term in Eqs. (5) and (6) has $d^{(2)}_{00}(\eta)$ angular dependence. Secondly, the observed line shape is rotor axis sensitive, in that different portions of Eqs. (5) and (6) are averaged to zero depending on the choice of ζ. Equations (10) and (11) indicate that rotation about an angle magic for $d^{(2)}_{00}(\zeta)$ (54.74°) provides a mixture of $d^{(4)}_{00}(\eta)$ and $d^{(2)}_{00}(\eta)$ angular dependence. The chief reduced matrix element contributor to the total line shape depends explicitly on the choice of ω_I, ω_S, ω_D, and ω_{rf} as seen in Figs. 3–6. MASS centerbands for these spin pairs corresponding to sample rotation about angles magic for $d^{(4)}_{00}(\zeta)$ (30.56° and 70.12°) are also included. Usually, single angle rotation about 54.74° provides the narrowest possible NMR line as it eliminates first order second rank interactions. However, in the ^{13}C–^{1}H case, rotation about 30.56° or 70.12° produces a narrower line, assuming that there is no CSA. This narrowing results from a combination of the frequency coefficients in Eqs. (5) and (6) and the $d^{(2)}_{02}(\zeta)d^{(2)}_{00}(\eta)$ term. These second order effects are usually not a nuisance in conventional ^{1}H decoupling experiments, as the predicted broadening is on the order of spectrometer resolution (0.1 ppm). However, such effects become important when considering decoupling experiments on other nuclei.

The presence of powder patterns under conditions of MASS also make it difficult to probe the isotropic shift of the magnetic resonance signal. The isotropic or average shift of the I spin (in units of Hz) while correcting for Bloch–Siegert effects is obtained by averaging the angular dependences in Eq. (7) over a solid angle of 4π.[17]

$$\Delta\omega_{\rm iso}=\omega_I+\frac{\omega_D^2}{20}\left(\frac{3}{\omega_I}+\frac{6}{\omega_I+\omega_S}+\frac{1}{\omega_I-\omega_S}\right). \tag{12}$$

In the case of methine ^{13}C–^{1}H pairs, Eq. (12) predicts a shift of $\Delta\omega_{ISO}/2\pi\approx0.46$ ppm at 15 MHz for ^{13}C and 0.04 ppm at 50 MHz. This corresponds to a difference of 0.42 ppm between the low field and high field measurements which is somewhat larger than the values provided by VanderHart.[1] This discrepancy can be accounted for by considering that ^{13}C–^{1}H couplings are always averaged to some extent. Whereas a typical ^{13}C–^{1}H dipolar coupling is calculated as 23 kHz using $\omega_D=\gamma_I\gamma_S\hbar/\mathbf{r}^3_{IS}$ and $\mathbf{r}_{C-H}=1.09$ Å, experiments usually measure a value 20% smaller due to motional averaging.[18] Employing a motionally averaged ^{13}C–^{1}H dipolar coupling of 18.4 kHz results in a calculated second order dipolar shift of 0.26 ppm, which is in much better agreement with the experimental observations. In this light, the agreement between measured and calculated second order shifts using the previous theory which included only the Ω_3 terms can be seen as somewhat fortuitous. This was realized by VanderHart who pointed out that the nominal dipolar coupling needed to account for the observed field dependent shifts was too large if one admitted to the usual degree of motional averaging.

Experimental measurement of such small lineshifts requires an accurate determination of the isotropic shift at a given field strength. Unfortunately, the presence of a line broadening mechanism dependent on the rf power may make such identification difficult. The effect of the second rank coupling of the applied rf decoupling field with the heteronuclear dipolar interaction can be seen most clearly by comparing expected MASS centerband line shapes with and without decoupling. Figure 7 shows both (a) ^{13}C–^{1}H and (b) ^{119}Sn–^{1}H MASS centerbands using the same dipolar coupling constants employed above. In these cases a rotation angle of $\zeta=54.74°$ and $\omega_{rf}/2\pi=60$ kHz was used. The rf power broadening is readily apparent in the

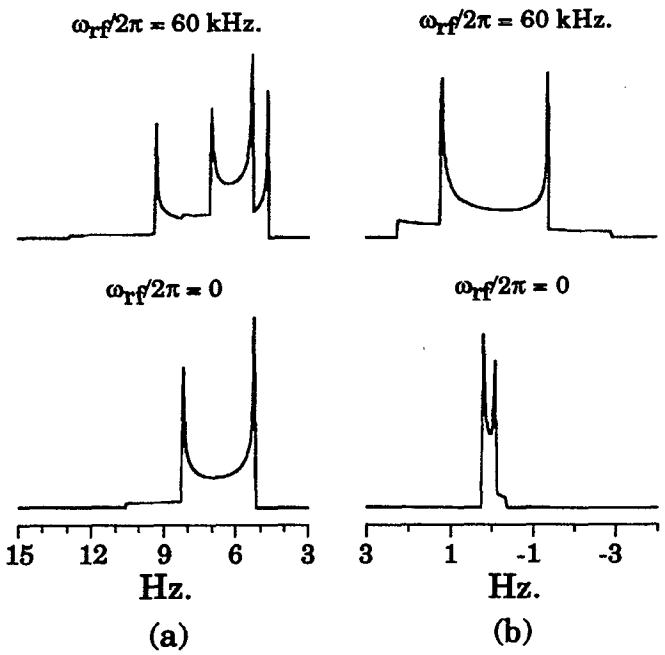

FIG. 7. (a) MASS centerband line shapes obtained with (top) and without decoupling ($\omega_{rf}/2\pi=60$ kHz) for the methine ^{13}C–^{1}H spin pair. (b) The line shapes corresponding to the ^{119}Sn–^{1}H spin pair under identical conditions. The ^{119}Sn line shapes clearly indicate the presence of the pseudo-power broadening. The decoupled line shape is ten times wider than the undecoupled resonance.

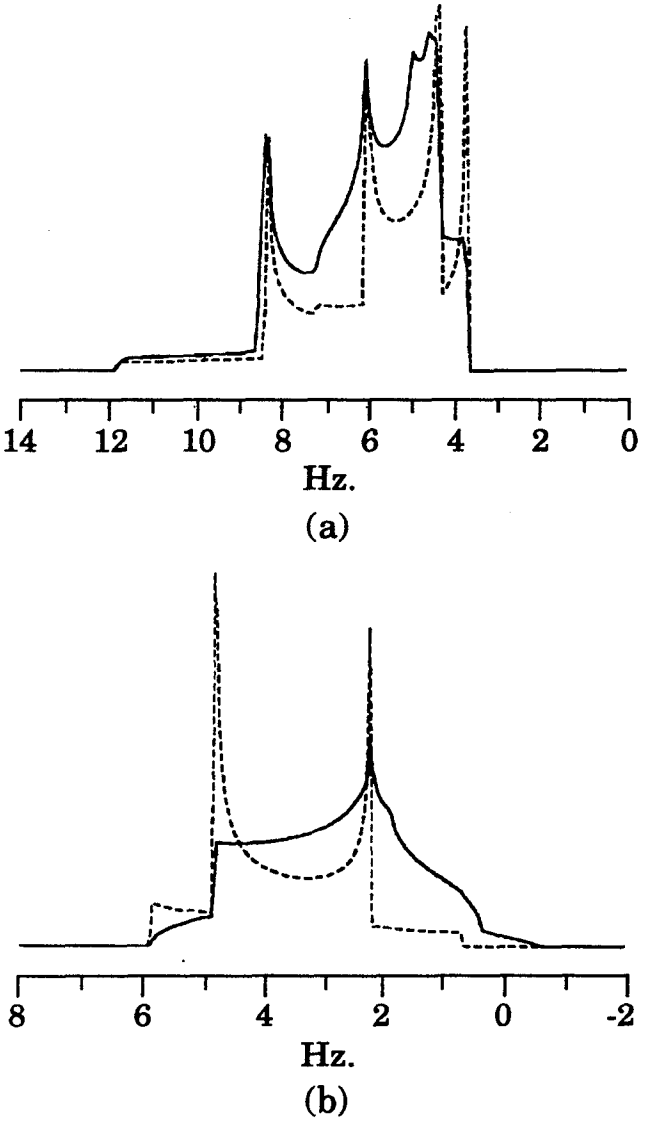

FIG. 8. Conventional MASS centerbands showing the effects of rf inhomogeneity on the expected line shapes for the (a) methine ^{13}C–^{1}H spin pair and the (b) ^{119}Sn–^{1}H spin pair in $SnHR_3$ at $B=1.4$ T and $\omega_{rf}/2\pi=60$ kHz. The z component of the magnetic field as a function of position inside a solenoid coil having a diameter of 5 mm and a length of 7.5 mm was used to estimate the decoupling field strength across a sample filling the entire coil volume.

^{119}Sn–^{1}H dipolar coupled spin pair. The linewidth without decoupling is almost ten times narrower than with decoupling. This dramatic increase in linewidth as a function of ω_{rf} for the ^{119}Sn–^{1}H spin pair is a direct result of the negative gyromagnetic ratio of ^{119}Sn. The most important term in Eqs. (10) and (11) in this case is linear in ω_{rf}. Other terms in Eq. (10) dominate for other spin pairs such as ^{13}C–^{1}H, and the decoupled linewidth more closely resembles that of the undecoupled resonance.

The existence of this rf power broadening following mechanical sample rotation, suggests that rf inhomogeneity will also be a problem in accurately assigning the isotropic shift. An inhomogeneous distribution in rf throughout a sample will provide a corresponding spread in both pseudo-power broadening and Bloch–Siegert shifts. Insight into the effects of rf inhomogeneity on the MASS centerbands for $\zeta=54.74°$ can be obtained from Fig. 8. Figure 8 shows the MASS centerband including Bloch–Siegert effects with (solid line) and without inhomogeneous rf field for the same ^{13}C–^{1}H and ^{119}Sn–^{1}H pairs used above. This figure clearly illustrates that rf inhomogeneity significantly alters MASS centerbands, especially in the ^{119}Sn–^{1}H case, which is unfortunate as the second order effects predicted by this theory are more easily realized in this system.

Given the steady increase in field strengths that are being routinely employed in CP-MAS experiments, it is natural to ask how high a field is necessary to render the effects discussed here insignificant. In the case of ^{13}C–^{1}H it can be seen from MASS centerband calculations that above a field strength of 4.7 T the excess linewidth resulting from *pseudo-power* broadening becomes insignificant in comparison to 0.1 ppm. This is about the resolution one can expect in CP-MAS experiments given other linebroadening factors such as magnetic susceptibility effects, off resonance ^{1}H decoupling contributions or simple site to site variations in chemical shifts due to lattice disorder.[19] For the ^{119}Sn–^{1}H spin pair these effects persist only to a field strength of 2.34 T.

CONCLUSIONS

We have provided a more complete description of the problem of second order dipolar shifts in high resolution solid state NMR spectroscopy. The suggestion that the dominant features of the shift were associated with the Ω_3 elements of the dipolar Hamiltonian is largely correct for the specific case of ^{13}C NMR with high power decoupling. These specific terms dominate because the denominators associated with the different terms in the effective Hamiltonian are large except for the term containing $|\Omega_3|^2$. However, this is not generally the case. In ^{119}Sn–^{1}H systems where the denominators are the smallest should have drastically different field dependent isotropic resonance shifts and powder line shapes. These second order shifts will survive in both decoupled and coupled systems. The shifts (0.42 ppm for ^{13}C–^{1}H) are large enough to be important in the analysis of liquid crystal data.

ACKNOWLEDGMENTS

Support of this work by the U. S. Department of Energy under Grant No. DE-FG22-91PC91285 is gratefully acknowledged. K.W.Z. would also like to acknowledge stimulating discussions with David L. VanderHart.

APPENDIX

The time dependent Hamiltonian matrix, $\mathscr{H}_R(t)$ is shown below where

$$\mathcal{H}_R(t) = \mathcal{H}_R^{(0)} + \mathcal{H}(t)$$

$$\mathcal{H}_R^{(0)} = \begin{array}{c} \\ \langle\alpha\alpha| \\ \langle\alpha\beta| \\ \langle\beta\alpha| \\ \langle\beta\beta| \end{array} \begin{array}{c} \begin{array}{cccc} |\alpha\alpha\rangle & |\alpha\beta\rangle & |\beta\alpha\rangle & |\beta\beta\rangle \end{array} \\ \begin{pmatrix} -\frac{\omega_I}{2}+\frac{\Omega_1}{4} & -\frac{\omega_{rf}}{2} & \frac{\Omega_3}{2} & 0 \\ -\frac{\omega_{rf}}{2} & -\frac{\omega_I}{2}-\frac{\Omega_1}{4} & 0 & -\frac{\Omega_3}{2} \\ \frac{\Omega_3^*}{2} & 0 & \frac{\omega_I}{2}-\frac{\Omega_1}{4} & -\frac{\omega_{rf}}{2} \\ 0 & -\frac{\Omega_3^*}{2} & -\frac{\omega_{rf}}{2} & \frac{\omega_I}{2}+\frac{\Omega_1}{4} \end{pmatrix} \end{array},$$

$$\mathcal{H}(t) = \begin{array}{c} \\ \langle\alpha\alpha| \\ \langle\alpha\beta| \\ \langle\beta\alpha| \\ \langle\beta\beta| \end{array} \begin{array}{c} \begin{array}{cccc} |\alpha\alpha\rangle & |\alpha\beta\rangle & |\beta\alpha\rangle & |\beta\beta\rangle \end{array} \\ \begin{pmatrix} 0 & -\frac{\omega_{rf}}{2}e^{-2i\omega_S t}+\frac{\Omega_3}{2}e^{-i\omega_S t} & -\frac{\gamma\omega_{rf}}{2}(e^{-i\omega_S t}+e^{i\omega_S t}) & \Omega_4 e^{-i\omega_S t} \\ -\frac{\omega_{rf}}{2}e^{2i\omega_S t}+\frac{\Omega_3^*}{2}e^{i\omega_S t} & 0 & \Omega_2 e^{i\omega_S t} & -\frac{\gamma\omega_{rf}}{2}(e^{-i\omega_S t}+e^{i\omega_S t}) \\ -\frac{\gamma\omega_{rf}}{2}(e^{-i\omega_S t}+e^{i\omega_S t}) & \Omega_2 e^{-i\omega_S t} & 0 & -\frac{\omega_{rf}}{2}e^{-2i\omega_S t}-\frac{\Omega_3}{2}e^{-i\omega_S t} \\ \Omega_4^* e^{i\omega_S t} & -\frac{\gamma\omega_{rf}}{2}(e^{-i\omega_S t}+e^{i\omega_S t}) & -\frac{\omega_{rf}}{2}e^{2i\omega_S t}-\frac{\Omega_3^*}{2}e^{i\omega_S t} & 0 \end{pmatrix} \end{array}.$$

[1] D. L. VanderHart, J. Chem. Phys. **84**, 1196 (1986).
[2] (a) V. Royden, Phys. Rev. **96**, 3300 (1954); (b) A. L. Bloom and J. N. Shoolery, *ibid.* **97**, 1955.
[3] (a) E. R. Andrews, A. Bradbury, and R. G. Eades, Nature, **182**, 1659 (1958); (b) *ibid.* **183**, 1802 (1959); (c) I. J. Lowe, Phys. Rev. Lett **2**, 285 (1959); (d) M. M. Maricq and J. S. Waugh, J. Chem. Phys. **70**, 3300 (1979).
[4] W. L. Earl and D. L. VanderHart, J. Magn. Reson. **48**, 35 (1982).
[5] (a) J. H. Shirley, Phys. Rev. B **138**, 979 (1965); (b) G. Goelman, S. Vega, and D. B. Zax, Phys. Rev. A **39**, 5725 (1989); (c) Y. Zur and S. Vega, J. Chem. Phys. **79**, 548 (1983).
[6] (a) C. P. Slichter, *Principles of Magnetic Resonance* (Springer-Verlag, New York, 1990), p. 66; (b) A. Abragam and M. Goldman, *Nuclear Magnetism, Order and Disorder* (Oxford Science, New York, 1982), p. 2; (c) R. K. Harris, *Nuclear Magnetic Resonance Spectroscopy* (Longman Group LTD, Hong Kong, 1987), p. 97.
[7] A. Abragam, *Principles of Nuclear Magnetism* (Oxford University, New York, 1961), p. 531.
[8] C. Cohen-Tannoudji, B. Diu, and F. Laloe, *Quantum Mechanics* (Wiley, New York, 1977), p. 1340.
[9] (a) S. R. Hartmann and E. L. Hahn, Phys. Rev. **128**, 2042 (1962); (b) A. Pines, M. G. Gibby, and J. S. Waugh, J. Chem. Phys. **56**, 1776 (1972); (c) **59**, 569 (1973); (d) Chem. Phys. Lett. **15**, 373 (1972).
[10] (a) G. Goelman, S. Vega, and D. B. Zax, Phys. Rev. A **39**, 5725

(1989); (b) M. M. Maricq, Phys. Rev. B **25**, 6622 (1982).
[11] G. Goelman, D. B. Zax, and S. Vega, J. Chem. Phys. **87**, 31 (1987).
[12] C. Cohen-Tannoudji, B. Diu, and F. Laloe, *Quantum Mechanics* (Wiley, New York, 1977), p. 122.
[13] (a) C. Cohen-Tannoudji, B. Diu, and F. Laloe, *Quantum Mechanics* (Wiley, New York, 1977), p. 1299; (b) W. H. Louisell, *Quantum Statistical Properties of Radiation* (Wiley Interscience, New York, 1990), p. 63.
[14] F. Bloch and A. Siegert, Phys. Rev. **57**, 552 (1940).
[15] (a) T. G. Oas, R. G. Griffin, and M. H. Levitt, J. Chem. Phys. **89**, 692 (1988); (b) M. G. Munowitz and R. G. Griffin, *ibid.* **76**, 2848 (1982).
[16] (a) H. J. Behrens, and B. Schnabel, Physica B **114**, 185 (1982); (b) K. T. Mueller, B. Q. Sun, G. C. Chingas, J. W. Zwanziger, T. Terao, and A. Pines, J. Magn. Reson. **86**, 470 (1990); (c) E. Kundla, A. Samoson, and E. Lippmaa, Chem. Phys. Lett. **83**, 229 (1981).
[17] C. P. Slichter, *Principles of Magnetic Resonance* (Springer-Verlag, New York, 1990), p. 261.
[18] J. Schaefer, E. O. Stejskal, R. A. McKay, and W. T. Dixon, Macromolecules **17**, 1479 (1984).
[19] H. Eckert, Ber. Bunsenges. Phys. Chem. **94**, 1062 (1990).